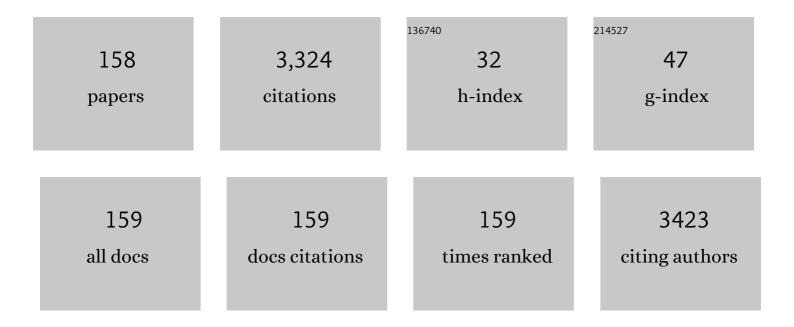
Qianming Wang

List of Publications by Year in descending order

Source: https://exaly.com/author-pdf/8519706/publications.pdf Version: 2024-02-01



#	Article	IF	CITATIONS
1	Novel luminescent terbium molecular-based hybrids with modified meta-aminobenzoic acid covalently bonded with silica. Journal of Materials Chemistry, 2004, 14, 2450.	6.7	203
2	Optical and electrochemical responses of an anthrax biomarker based on single-walled carbon nanotubes covalently loaded with terbium complexes. Chemical Communications, 2011, 47, 12521.	2.2	109
3	Signal transduction from small particles: Sulfur nanodots featuring mercury sensing, cell entry mechanism and in vitro tracking performance. Chemical Engineering Journal, 2020, 382, 122907.	6.6	108
4	Synergistic regulation of effective detection for hypochlorite based on a dual-mode probe by employing aggregation induced emission (AIE) and intramolecular charge transfer (ICT) effects. Chemical Engineering Journal, 2019, 368, 157-164.	6.6	74
5	Imaging two targets in live cells based on rational design of lanthanide organic structure appended carbon dots. Carbon, 2015, 93, 671-680.	5.4	65
6	Stable Triple Cation Perovskite Precursor for Highly Efficient Perovskite Solar Cells Enabled by Interaction with 18C6 Stabilizer. Advanced Functional Materials, 2020, 30, 1908613.	7.8	65
7	Reversible Terbium Luminescent Polyelectrolyte Hydrogels for Detection of H2PO4â^'and HSO4â^'in Water. Inorganic Chemistry, 2011, 50, 2953-2956.	1.9	64
8	Oxidative deoximation reaction induced recognition of hypochlorite based on a new fluorescent lanthanide-organic framework. Chemical Engineering Journal, 2018, 351, 364-370.	6.6	63
9	A New Fluoride Luminescence Quencher Based on a Nanostructured Covalently Bonded Terbium Hybrid Material. Journal of Physical Chemistry C, 2010, 114, 13879-13883.	1.5	61
10	Solventâ€Assisted Lowâ€Temperature Crystallization of SnO ₂ Electronâ€Transfer Layer for Highâ€Efficiency Planar Perovskite Solar Cells. Advanced Functional Materials, 2019, 29, 1900557.	7.8	59
11	New lanthanide ternary complex system in electrospun nanofibers: Assembly, physico-chemical property and sensor application. Chemical Engineering Journal, 2019, 358, 67-73.	6.6	59
12	Ratiometric Fluorescence Platform Based on Modified Silicon Quantum Dots and Its Logic Gate Performance. Inorganic Chemistry, 2018, 57, 8866-8873.	1.9	58
13	Highly efficient and selective turn-off quenching of ligand-sensitized luminescence from europium imidazo[4,5-f]-1,10-phenanthroline complex by fluoride ion. Journal of Photochemistry and Photobiology A: Chemistry, 2009, 206, 124-128.	2.0	47
14	Optimization of hierarchical structure and nanoscale-enabled plasmonic refraction for window electrodes in photovoltaics. Nature Communications, 2016, 7, 12825.	5.8	46
15	Modulation of assembly and disassembly of a new tetraphenylethene based nanosensor for highly selective detection of hyaluronidase. Sensors and Actuators B: Chemical, 2018, 276, 95-100.	4.0	46
16	2D MnO ₂ nanosheets generated signal transduction with 0D carbon quantum dots: synthesis strategy, dual-mode behavior and glucose detection. Nanoscale, 2019, 11, 13058-13068.	2.8	45
17	Smart choice of carbon dots as a dual-mode onsite nanoplatform for the trace level detection of Cr2O72 Dyes and Pigments, 2019, 163, 102-110.	2.0	44
18	Terbium hybrid particles with spherical shape as luminescent probe for detection of Cu2+ and Fe3+ in water. Analytica Chimica Acta, 2011, 708, 111-115.	2.6	41

#	Article	IF	CITATIONS
19	Mussel chemistry assembly of a novel biosensing nanoplatform based on polydopamine fluorescent dot and its photophysical features. Chemical Engineering Journal, 2018, 342, 331-338.	6.6	41
20	Role of novel silicon nanoparticles in luminescence detection of a family of antibiotics. RSC Advances, 2015, 5, 27458-27463.	1.7	40
21	An unusual way to luminescent terbium molecular-level hybrid materials: Modified methyl benzoic acid covalently bonded with silica as a bridge. Journal of Materials Research, 2005, 20, 592-598.	1.2	39
22	A Practical ITO Replacement Strategy: Sputteringâ€Free Processing of a Metallic Nanonetwork. Advanced Materials Technologies, 2017, 2, 1700061.	3.0	39
23	A luminescent lanthanide complex-based anion sensor with electron-donating methoxy groups for monitoring multiple anions in environmental and biological processes. Spectrochimica Acta - Part A: Molecular and Biomolecular Spectroscopy, 2012, 96, 387-394.	2.0	38
24	Extension of Novel Lanthanide Luminescent Mesoporous Nanostructures to Detect Fluoride. Inorganic Chemistry, 2014, 53, 1530-1536.	1.9	38
25	Emission response towards three anions (Fâ^', HSO4â^' and AcOâ^') by a luminescent europium ternary complex with a 2-arylimidazole-1,10-phenanthroline conjugate. Photochemical and Photobiological Sciences, 2010, 9, 791-795.	1.6	36
26	Multiple irradiation triggered the formation of luminescent LaVO4: Ln3+ nanorods and in cellulose gels. CrystEngComm, 2012, 14, 4786.	1.3	36
27	Two emissive cellulose hydrogels for detection of nitrite using terbium luminescence. Sensors and Actuators B: Chemical, 2012, 173, 833-838.	4.0	35
28	Equivalent cation substitution-triggered highly efficient Mn4+ red emission in double-perovskite type (Ba, Sr)2(Gd, La, Y, Lu)(Nb, Sb)O6:Mn4+ solid solution phosphors and photophysical studies. Chemical Engineering Journal, 2021, 424, 130571.	6.6	35
29	Spectroscopic analysis and in vitro imaging applications of a pH responsive AIE sensor with a two-input inhibit function. Chemical Communications, 2015, 51, 12060-12063.	2.2	34
30	Lanthanide induced formation of novel luminescent alginate hydrogels and detection features. Carbohydrate Polymers, 2015, 133, 19-23.	5.1	34
31	Fluorescentâ€based Solid Sensor for HSO ₄ ^{â^'} in Water. Photochemistry and Photobiology, 2010, 86, 1191-1196.	1.3	33
32	Systematic studies for the novel synthesis of nano-structured lanthanide fluorides. Chemical Engineering Journal, 2014, 250, 190-197.	6.6	33
33	Concentrated solar irradiation protocols for the efficient synthesis of tri-color emissive carbon dots and photophysical studies. Journal of Materials Chemistry C, 2018, 6, 13013-13022.	2.7	33
34	Efficient and visual monitoring of cerium (III) ions by green-fluorescent carbon dots and paper-based sensing. Spectrochimica Acta - Part A: Molecular and Biomolecular Spectroscopy, 2019, 206, 240-245.	2.0	33
35	Efficient Energy Transfer from Trap Levels to Eu ³⁺ Leads to Antithermal Quenching Effect in High-Power White Light-Emitting Diodes. Inorganic Chemistry, 2020, 59, 15514-15525.	1.9	32
36	Two optically active molybdenum disulfide quantum dots as tetracycline sensors. Materials Chemistry and Physics, 2016, 178, 82-87.	2.0	31

#	Article	IF	CITATIONS
37	Rapid conversion from common precursors to carbon dots in large scale: Spectral controls, optical sensing, cellular imaging and LEDs application. Journal of Colloid and Interface Science, 2020, 580, 88-98.	5.0	31
38	A targetable fluorescent sensor for hypochlorite based on a luminescent europium complex loaded carbon nanotube. Analyst, The, 2012, 137, 1872.	1.7	30
39	Colossal Figure of Merit in Transparentâ€Conducting Metallic Ribbon Networks. Advanced Materials Technologies, 2016, 1, .	3.0	29
40	Prevailing paradigms in novel lanthanide optical probes from molecular complexes to hybrid materials. Sensors and Actuators B: Chemical, 2017, 245, 622-640.	4.0	29
41	Luminescence modulation of two individual fluorophores over a wide pH range and intracellular studies. Dyes and Pigments, 2018, 150, 151-157.	2.0	29
42	Effects of multiple irradiations on luminescent materials and energy savings – A case study for the synthesis of BaMO 4 : Ln 3+ (MÂ=ÂW, Mo; LnÂ=ÂEu, Tb) phosphors. Energy, 2014, 64, 551-556.	4.5	28
43	Anion/Cation Induced Optical Switches Based on Luminescent Lanthanide (Tb ³⁺ and) Tj ETQq1 1 0	.784314 rş 1.3	gBŢ_/Overloch
44	Novel lanthanide pH fluorescent probes based on multiple emissions and its visible-light-sensitized feature. Analytica Chimica Acta, 2014, 839, 51-58.	2.6	27
45	Chemical sensing failed by aggregation-caused quenching? A case study enables liquid/solid two-phase determination of N2H4. Chemical Engineering Journal, 2021, 415, 128975.	6.6	26
46	Molten salt synthesis, characterization, and luminescence properties of GdNbO4/LuTaO4:Eu3+ phosphors. Materials Research Bulletin, 2013, 48, 2771-2775.	2.7	25
47	Fluorometric determination of dopamine by using a terbium (III) inorganic-organic network. Mikrochimica Acta, 2017, 184, 2275-2280.	2.5	25
48	Tetracycline Generated Red Luminescence Based on a Novel Lanthanide Functionalized Layered Double Hydroxide Nanoplatform. Journal of Agricultural and Food Chemistry, 2019, 67, 3871-3878.	2.4	25
49	Aggregation Induced Emission Mediated Controlled Release by Using a Built-In Functionalized Nanocluster with Theranostic Features. Journal of Medicinal Chemistry, 2016, 59, 410-418.	2.9	24
50	Precise control for the aggregation and deaggregation with the aid of a tetraphenylethylene derivative: Luminescence modulation and sensing performance. Dyes and Pigments, 2020, 172, 107844.	2.0	24
51	Green anhydrous assembly of carbon dots via solar light irradiation and its multi-modal sensing performance. Dyes and Pigments, 2019, 165, 287-293.	2.0	23
52	A novel self-calibrating strategy for real time monitoring of formaldehyde both in solution and solid phase. Journal of Hazardous Materials, 2020, 386, 121883.	6.5	23
53	Smart pH sensitive luminescent hydrogel based on Eu(III) \hat{I}^2 -diketonate complex and its enhanced photostability. Journal of Photochemistry and Photobiology A: Chemistry, 2009, 201, 87-90.	2.0	22
54	Preparation of one-dimensional La2â^'Gd (MoO4)3â^'(WO4) : Eu3+ amorphous materials by multiple irradiations and in polymeric gels. Chemical Engineering Journal, 2014, 244, 350-354.	6.6	22

#	Article	IF	CITATIONS
55	A New Co-Substitution Strategy as a Model to Study a Rare-Earth-Free Spinel-Type Phosphor with Red Emissions and Its Application in Light-Emitting Diodes. Inorganic Chemistry, 2020, 59, 433-442.	1.9	22
56	Luminescent Cu2+ Probes Based on Rare-Earth (Eu3+ and Tb3+) Emissive Transparent Cellulose Hydrogels. Journal of Fluorescence, 2012, 22, 1581-1586.	1.3	21
57	3D honeycomb NiCo2S4 @ Ni(OH)2 nanosheets for flexible all-solid-state asymmetric supercapacitors with enhanced specific capacitance. Journal of Alloys and Compounds, 2019, 790, 693-702.	2.8	21
58	Optical detection of anthrax biomarkers in an aqueous medium: the combination of carbon quantum dots and europium ions within alginate hydrogels. Journal of Materials Science, 2019, 54, 2526-2534.	1.7	21
59	Synthesis of luminescent YVO4:Eu3+ submicrometer crystals through hydrogels as directing agents. Materials Chemistry and Physics, 2012, 135, 451-456.	2.0	20
60	Electrochemical signal response for vitamin B1 using terbium luminescent nanoscale building blocks as optical sensors. Sensors and Actuators B: Chemical, 2013, 188, 1176-1182.	4.0	20
61	Molecular imaging of biothiols and in vitro diagnostics based on an organic chromophore bearing a terbium hybrid probe. Dalton Transactions, 2016, 45, 7435-7442.	1.6	20
62	Nucleophilic Additionâ€īriggered Lanthanide Luminescence Allows Detection of Amines by Eu(thenoyltrifluoroacetone) ₃ . Photochemistry and Photobiology, 2012, 88, 840-843.	1.3	19
63	Supersonic microwave co-assistance (SMC) efficient synthesis of red luminescent Eu3+ activated silver molybdates and their phase-dependent evolution processes. CrystEngComm, 2013, 15, 5668.	1.3	19
64	Realization of an Optical Thermometer via Structural Confinement and Energy Transfer. Inorganic Chemistry, 2021, 60, 19315-19327.	1.9	19
65	Eu3+ chelate with phenanthroline derivative gives selective emission responses to Cu(II) ions. Journal of Organometallic Chemistry, 2011, 696, 829-831.	0.8	18
66	Dibenzoyl-l-cystine as organic directing agent for assembly of visible-light-sensitized luminescent AgGd(MoO4)2:Eu3+ nanowires. Materials Research Bulletin, 2012, 47, 856-860.	2.7	18
67	Terbium-containing graphene oxide and its opto-electrochemical response for hypochlorite in water. Carbon, 2013, 58, 232-237.	5.4	18
68	2-(3-Pyridyl)imidazole-4,5-dicarboxylic acid based lanthanide luminescent anion sensor. Solid State Sciences, 2011, 13, 1687-1691.	1.5	17
69	Relationship between crystal structure and luminescent properties of novel red emissive BiVO4:Eu3+ and its photocatalytic performance. Journal of Nanoparticle Research, 2012, 14, 1.	0.8	17
70	Assembly of novel Tb3+/Eu3+ sensitized cellulose gels and their emission behaviors. Cellulose, 2013, 20, 841-848.	2.4	17
71	Effective assembly of a novel aluminum-oxynitride BaAl11O16N activated by Eu2+ and Mn2+ via salt-flux assistance and its photophysical investigation. Journal of Alloys and Compounds, 2019, 787, 96-103.	2.8	17
72	Fluorinated interfacial layers in perovskite solar cells: efficient enhancement of the fill factor. Journal of Materials Chemistry A, 2020, 8, 16527-16533.	5.2	17

#	Article	IF	CITATIONS
73	Luminescence recognition behavior concerning different anions by lanthanide complex equipped with electron-withdraw groups and in PMMA matrix. Synthetic Metals, 2010, 160, 1780-1786.	2.1	16
74	Photophysical studies of novel lanthanide (Eu3+ and Tb3+) luminescent hydrogels. Inorganic Chemistry Communication, 2011, 14, 515-518.	1.8	16
75	CdMoO4:Eu3+ micro-sized luminescent particles synthesis and photo-catalytic performance. Inorganica Chimica Acta, 2013, 408, 59-63.	1.2	16
76	A Novel Luminescent Organogel Containing Dysprosium Ions Quenched by Gel-to-sol Transition. Chemistry Letters, 2008, 37, 430-431.	0.7	15
77	Diverse reactivity to hypochlorite and copper ions based on a novel Schiff base derived from vitamin B6 cofactor. Journal of Molecular Liquids, 2020, 319, 114124.	2.3	15
78	Establishment of a new molecular model for mercury determination verified by single crystal X-ray diffraction, spectroscopic analysis and biological potentials. Chinese Chemical Letters, 2021, 32, 87-91.	4.8	15
79	Composition adjustment verifies structure-property correlation in narrow-band green-emitting Zn4-Mg B6O13: Mn2+ phosphor. Journal of Luminescence, 2021, 236, 118101.	1.5	15
80	Polyurethane-based Eu(iii) luminescent foam as a sensor for recognizing Cu2+ in water. Analytical Methods, 2013, 5, 6045.	1.3	14
81	Thiazole derivative based terbium(III) covalent silica nanosphere and its sensing property. Inorganica Chimica Acta, 2013, 394, 127-131.	1.2	14
82	Establishment of a new analytical platform for glucose detection based on a terbium containing silica hybrid nanosensor. Applied Surface Science, 2018, 462, 883-889.	3.1	14
83	Sequential determination of cerium (IV) ion and ascorbic acid via a novel organic framework: A subtle interplay between intramolecular charge transfer (ICT) and aggregated-induced-emission (AIE). Journal of Molecular Liquids, 2020, 304, 112705.	2.3	14
84	Recognition of H2PO 4 - and Cu2+ in Water by Luminescent Terbium Silica Xerogel. Journal of Fluorescence, 2011, 21, 1117-1122.	1.3	13
85	Influence of processing parameters on the luminescence of Eu3+ activated YTa1â ^{~3} xNbxO4 phosphors by a molten salt method. Journal of Luminescence, 2015, 158, 417-421.	1.5	13
86	Simultaneously enhanced J _{sc} and FF by employing two solution-processed interfacial layers for inverted planar perovskite solar cells. RSC Advances, 2017, 7, 39523-39529.	1.7	13
87	Carbazole based new organic dye recognizes hydrazine and hydrogen sulfide via signal difference protocols. Dyes and Pigments, 2020, 181, 108545.	2.0	13
88	Design and evaluation of highly sensitive luminescent terbium sensor for hypochlorite in water. Journal of Sol-Gel Science and Technology, 2011, 60, 159-163.	1.1	12
89	Design of europium doped SiO2–TiO2 hybrids as novel luminescent photocatalyst. Journal of Luminescence, 2012, 132, 1639-1641.	1.5	12
90	Aggregation-induced-emission (AIE) directed assembly of a novel responsive nanoprobe for dual targets sensing. Materials Science and Engineering C, 2019, 99, 1092-1098.	3.8	12

#	Article	IF	CITATIONS
91	Conversion of Lewis acid-base interaction into readable emission outputs by novel terbium hybrid nanosphere. Dyes and Pigments, 2015, 112, 239-244.	2.0	11
92	Nondestructive Transfer Strategy for High-Efficiency Flexible Perovskite Solar Cells. ACS Applied Materials & Interfaces, 2019, 11, 47003-47007.	4.0	11
93	Near-infrared emission tracks inter-individual variability of carboxylesterase-2 via a novel molecular substrate. Mikrochimica Acta, 2020, 187, 313.	2.5	11
94	Luminescent terbium(iii) complex-based titania sensing material for fluoride and its photocatalytic properties. Photochemical and Photobiological Sciences, 2012, 11, 738.	1.6	10
95	LaPO4:Eu3+ in situ formed in polymeric gels and its photophysical properties. Optical Materials, 2012, 34, 1019-1022.	1.7	10
96	Smart 0D nanomaterials assembled by green luminescent terbium hybrids for the detection of tryptophan. Journal of Nanoparticle Research, 2013, 15, 1.	0.8	10
97	An intelligent copper(II) luminescent sensor using europium narrow emissions based on titania hybrid material. Optical Materials, 2014, 36, 1520-1524.	1.7	10
98	Soft Matter Anion Sensing Based on Lanthanide (Eu3+and TB3+) Luminescent Hydrogels. Soft Materials, 2014, 12, 98-102.	0.8	10
99	Extensive studies of host lattices and activators in lanthanide phosphors based on efficient synthesis. Journal of Alloys and Compounds, 2016, 676, 292-298.	2.8	10
100	Structural-property correlations of all-inorganic CsPbBr3 perovskites via synergetic controls by PbBr2, 2-mercapto-3-methyl-4-thiazoleacetic acid and water. Chemical Engineering Journal, 2022, 428, 131117.	6.6	10
101	Near-infrared Luminescence from Ytterbium(III) Ternary Complexes by Visible-light Excitation of Attached Chlorophyll Derivatives. Chemistry Letters, 2009, 38, 648-649.	0.7	9
102	Arginine-responsive terbium luminescent hybrid sensors triggered by two crown ether carboxylic acids. Materials Science and Engineering C, 2013, 33, 5090-5094.	3.8	9
103	Template synthesis, structure, optical and catalytic properties derived from novel cadmium tungstates. Polyhedron, 2016, 113, 102-108.	1.0	9
104	Reinforcing effects of waterproof substrate on the photo-, thermal and pH stabilities of perovskite nanocrystals. Journal of Alloys and Compounds, 2020, 817, 152693.	2.8	9
105	Extension of Spectral Shift Controls from Equivalent Substitution to an Energy Migration Model Based on Eu ²⁺ /Tb ³⁺ -Activated Ba _{4–<i>x</i>} Sr _{<i>x</i>} Gd _{3–<i>x</i>} Lu _{<i>x</i>} Na <sub Phosphors. Inorganic Chemistry. 2021. 60. 16507-16517.</sub 	>3	(PO ² _{4<}
106	Micro-Meter Size Organogelator with Tri-Color Luminescence (Blue, Green and Red) Activated by Dy3+, Tb3+ and Eu3+ ions. Journal of Fluorescence, 2009, 19, 793-800.	1.3	8
107	Two novel europium (III) centered anion receptors and their naked eye detections. Synthetic Metals, 2012, 162, 1416-1420.	2.1	8
108	Ultrasonic-assisted microwave synthesis of luminescent V2O5/MgF2:Eu3+ and its catalytic properties. Materials Letters, 2013, 98, 12-14.	1.3	8

#	Article	IF	CITATIONS
109	Novel pH Induced Reversible Luminescent Lanthanide Hydrogels. Journal of Cluster Science, 2013, 24, 449-458.	1.7	7
110	Encapsulation of lanthanides in ternary l–Ill–VI AgInS2 nanocrystals and their physical properties. Materials Letters, 2015, 141, 225-227.	1.3	7
111	Two novel luminescent metallic based organic–inorganic functionalized silica hybrid materials. Synthetic Metals, 2015, 209, 262-266.	2.1	7
112	Detection of double analytes by employing new luminescent lanthanide probe. Journal of Molecular Structure, 2015, 1099, 204-208.	1.8	7
113	Assay of fluoride by a novel organic–inorganic mesoporous nanoâ€sized sensor. Luminescence, 2016, 31, 1125-1129.	1.5	7
114	Variable Emission Changes in Bi3+/Ln3+ (LnÂ=ÂEu, Sm, Dy) Co-doped Lutetium Vanadates (LuVO4). Journal of Electronic Materials, 2016, 45, 2974-2980.	1.0	7
115	Exploration of Sulfur-Containing Nanoparticles: Synthesis, Microstructure Analysis, and Sensing Potential. Inorganic Chemistry, 2022, 61, 4159-4170.	1.9	7
116	Anion/Cation (H2PO4â^' and Fe3+) induced dual luminescence quenching effect based on terbium solid sensor. Journal of Rare Earths, 2010, 28, 888-892.	2.5	6
117	Novel templates directed synthesis of YVO4: Eu3+ (red) and Y2O3–SiO2: Tb3+(green) phosphors. Journal of Luminescence, 2012, 132, 2822-2825.	1.5	6
118	Selective signaling of fluoride anion based on imidazole moieties. Luminescence, 2012, 27, 302-306.	1.5	6
119	Facile synthesis of lanthanide vanadates and their luminescent properties. Displays, 2015, 39, 6-10.	2.0	6
120	Easy assembly of visible light excited lanthanide containing edifices and structural origin. Dyes and Pigments, 2015, 119, 56-61.	2.0	6
121	Low molecular weight molecule induces the effective stabilization of CsPbBr3 in water. Journal of Molecular Liquids, 2020, 299, 112199.	2.3	6
122	Anion Responsive Dibenzoylâ€ <scp>l</scp> â€Cystine and Luminescent Lanthanide Soft Material. Photochemistry and Photobiology, 2011, 87, 641-645.	1.3	5
123	From molecule to complex: Design of smart fluorescent anion-sensors. Optical Materials, 2013, 35, 1157-1161.	1.7	5
124	Design of red/green emissive lanthanide activated nano-materials by supersonic and microwave co-irradiations. Optical Materials, 2013, 35, 1146-1150.	1.7	5
125	Novel europium (III)-gatifloxacin complex structure with dual functionality for pH sensing and metal recognition in aqueous environment. Optical Materials, 2016, 60, 1-5.	1.7	5
126	Two novel sol–gel-derived nanostructures and their hemoglobin sensing features. Journal of Sol-Gel Science and Technology, 2016, 77, 205-210.	1.1	5

#	Article	IF	CITATIONS
127	Multi-modal tracking dopamine using a hybrid inorganic-organic silver nanoparticle and its cellular imaging performance. Journal of Luminescence, 2018, 204, 394-400.	1.5	5
128	Two molecular-based optical switches: Synthesis and their anions responses. Materials Letters, 2014, 126, 162-164.	1.3	4
129	Slow release realized in 40Âmin? Assembly of lanthanide hydroxycarbonates and oxycarbonates based on multiple irradiations. Journal of Nanoparticle Research, 2014, 16, 1.	0.8	4
130	Two novel benzene sulfonamide-modified luminescent nanosystems and their sensing features. Journal of Sol-Gel Science and Technology, 2015, 76, 164-170.	1.1	4
131	Ionic liquid synthesis of luminescent nano-cubes and their microstructure characterization. Journal of Molecular Structure, 2015, 1091, 1-5.	1.8	4
132	Self-organized dysprosium-directed alginate hydrogels and its chemical features. Journal of Luminescence, 2016, 177, 290-294.	1.5	4
133	Spectroscopic studies of noble metal incorporated lanthanide vanadates and YF3:Tb3+ nanoclusters encapsulated in hybrid hydrogels. Journal of Alloys and Compounds, 2017, 727, 1142-1147.	2.8	4
134	Room-temperature synthesis of novel polymeric nanoclusterwith emissions and its Cu2+ recognition performance. Journal of Luminescence, 2019, 205, 142-147.	1.5	4
135	Determination of Hypochlorite via Fluorescence Change from Blue to Green Based on 4-(1ÂH-imidazo) Tj ETQq1	1 0. 7843	14 rgBT /Over
136	Surface recognition strategy via ascorbic acid-triggered decomposition of boron nitride-loaded cobalt oxyhydroxide nanosheets. Journal of Alloys and Compounds, 2021, 872, 159625.	2.8	4
137	Side-chain substituent effects on green luminescence of terbium activated hybrid xerogels. Solid State Sciences, 2009, 11, 1617-1620.	1.5	3
138	Facile synthesis of visible light excited La1-xGdxF3: Eu3+ micro-meter sphere using polyvinylpyrrolidone as a template. Journal of Rare Earths, 2010, 28, 285-288.	2.5	3
139	Design of new lanthanide pH switches based on a cross-linked poly(vinyl alcohol)/tetraethoxysilane hybrid matrix. Colloid and Polymer Science, 2015, 293, 2979-2984.	1.0	3
140	In vitro and in vivo studies of a chlorin-based carbon nanocarrier with photodynamic therapy features. Photochemical and Photobiological Sciences, 2018, 17, 1329-1336.	1.6	3
141	Study of Specific Interaction between bis(p-phenylene)-34-crown-10-based Substituted Macrocycle and Ni2+. Journal of Fluorescence, 2018, 28, 725-728.	1.3	3
142	Sodium sulfite leads to the formation of fluorescent organic nanoparticles: Regulation from aqueous solution, cellular pathway to security design patterns. Dyes and Pigments, 2020, 176, 108252.	2.0	3
143	Stepwise Assembly Protocols for the Rational Design of Lanthanide Functionalized Carbon Dots-Hydrogel and its Sensing Evaluation. Journal of Fluorescence, 2021, 31, 695-702.	1.3	3
144	Lanthanide Molecular Species Generated Fe3O4@SiO2-TbDPA Nanosphere for the Efficient Determination of Nitrite. Molecules, 2022, 27, 4431.	1.7	3

#	Article	IF	CITATIONS
145	Efficient photosensitization of terbium ions enabled by hydrolysis of siloxy groups in ligands with specific side-chains. Photochemical and Photobiological Sciences, 2011, 10, 60-65.	1.6	2
146	Study of Interactions Between Eu(thenoyltrifluoroacetonate)3 and a Photosynthetic Chlorophyllous Pigment. Journal of Solution Chemistry, 2011, 40, 320-326.	0.6	2
147	Ultrasound and Microwave Coassisted Synthesis and Luminescent Properties of (Ln = La, Gd;) Phosphors. Journal of Chemistry, 2013, 2013, 1-6.	0.9	2
148	Magnolol and honokiol included green emissive terbium sol–gel materials and their recognition behaviors. Journal of Sol-Gel Science and Technology, 2014, 69, 231-236.	1.1	2
149	Effective fabrication of lanthanide activated phosphors and photoluminescence studies. Journal of Alloys and Compounds, 2017, 697, 25-30.	2.8	2
150	Single optical sensor to multiple functions: Ratiometric sensing for SO32â^' and dual signal determination for copper (II). Spectrochimica Acta - Part A: Molecular and Biomolecular Spectroscopy, 2021, 249, 119219.	2.0	2
151	Determination of prostate-specific antigen via the assembly of a two-dimensional nanoplatform. Journal of Nanoparticle Research, 2022, 24, 1.	0.8	2
152	Photophysical properties of novel ferrocenyl quinoline derivatives with red emission in solutions and polymeric matrices. Chemical Papers, 2010, 64, .	1.0	1
153	Design and characterization of new lanthanide fluorides and their optical properties. Displays, 2014, 35, 273-278.	2.0	1
154	Manipulation of novel nano-prodrug composed of organic pigment-based hybrid network and its optical uses. Materials Science and Engineering C, 2017, 70, 9-14.	3.8	1
155	Artificial mimics of light-harvesting organic pigment via a double-perovskite structure (LiLa2SbO6:Bi3+, Mg2+, Mn4+) with single-composition and structure-activity relationship. Journal of Luminescence, 2021, 239, 118351.	1.5	1
156	Construction of Novel Terbium Green Emissive Gels and Their Unique Thermal Degradation Processes. Journal of Cluster Science, 2012, 23, 147-154.	1.7	0
157	Metallic Nanonetworks: A Practical ITO Replacement Strategy: Sputteringâ€Free Processing of a Metallic Nanonetwork (Adv. Mater. Technol. 8/2017). Advanced Materials Technologies, 2017, 2, .	3.0	0
158	Interfacial charge changes induce the responsive behavior of two analytes based on novel carbon nanomaterials. Surfaces and Interfaces, 2022, 32, 102112.	1.5	0